

## THE ENHS CORE BENCHMARK

**D. Barnes, M. Milosevic', H. Sagara, K. Wang, E. Greenspan, J. Vujic and Z. Shayer**

Dept. of Nuclear Engineering  
University of California  
Berkeley, CA 94720-1730  
gehud@nuc.berkeley.edu

**K. Grimm, and R. Hill**

Reactor Analysis Division  
Argonne National Laboratory  
9700 South Cass Av.  
Argonne, IL 60439-4842  
b23921@ra.anl.gov, b35456@ra.anl.gov

**S.G. Hong and Y.I. Kim**

Korea Atomic Energy Research Institute  
Yusong, Taejon 305-600  
Rep. of Korea  
hongsg@kaeri.re.kr, yikim1@kaeri.re.kr

### ABSTRACT

Benchmarking of computational tools for neutronic design and analysis of the lead-cooled fast reactor ENHS was undertaken. The computational tools benchmarked include the MOCUP code and data libraries in use at UC Berkeley, the well-established fast reactor neutronic design tools in use at ANL, and similar tools in use at KAERI but with different cross-section data sets. Inter-compared are  $k_{\text{eff}}$  evolution with burnup, effective one group  $\nu$  values and cross sections for fission and capture, burnup dependent inventory of fuel isotopes, reflector reactivity worth and space dependent burnup and peak neutron flux.

### 1. INTRODUCTION

The Encapsulated Nuclear Heat Source (ENHS) is a new lead-bismuth or lead cooled novel reactor concept for a nominal power of  $125\text{MW}_{\text{th}}$  [1,2]. One of its novel design features is its core; it is to use uniform composition fuel rods, have no blanket elements and is to operate for 20 effective full power years without refueling and with very small reactivity swing.

In lack of experimental benchmark of comparable hard spectrum lead-cooled cores, a computational benchmark has been defined by the ENHS project team to provide a reference design case (benchmark) against which each participant will be able to evaluate his/hers computational tools and data libraries. So far three organizations participated in the ENHS benchmark analysis. The purpose of this paper is to describe the ENHS benchmark problem and to inter-compare the results obtained.

### 2. COMPUTATIONAL BENCHMARK MODEL

The ENHS benchmark is shown in Figure 1. The material compositions for this reference problem are

given in Table I. The atomic number densities for composing materials are presented in Table II. The reactor thermal power is 250 MW and is constant for the entire life of the ENHS assumed to be 30 years. The average specific power is 6.12 W/gHM corresponding to an average linear heat rate of 120 W/cm. The core is assumed to be homogeneous and of annular cylindrical geometry.

The fuel is a metallic alloy of 90 w/o heavy metal (HM) and 10 w/o Zr. Its density is assumed to be 75% of the nominal density. The HM consists of 9.81 w/o Pu and 80.19 w/o U. The uranium is the depleted to 0.2 w/o  $^{235}\text{U}$ . The isotopic composition of the loaded plutonium is 67.2 w/o  $^{239}\text{Pu}$ , 21.7 w/o  $^{240}\text{Pu}$ , 6.4 w/o  $^{241}\text{Pu}$  and 4.7 w/o  $^{242}\text{Pu}$ . The clad is made of stainless steel having 17 w/o Cr, 14 w/o Ni, 2.8 w/o Mo and 1.5 w/o Mn; the rest is Fe. The coolant is lead.

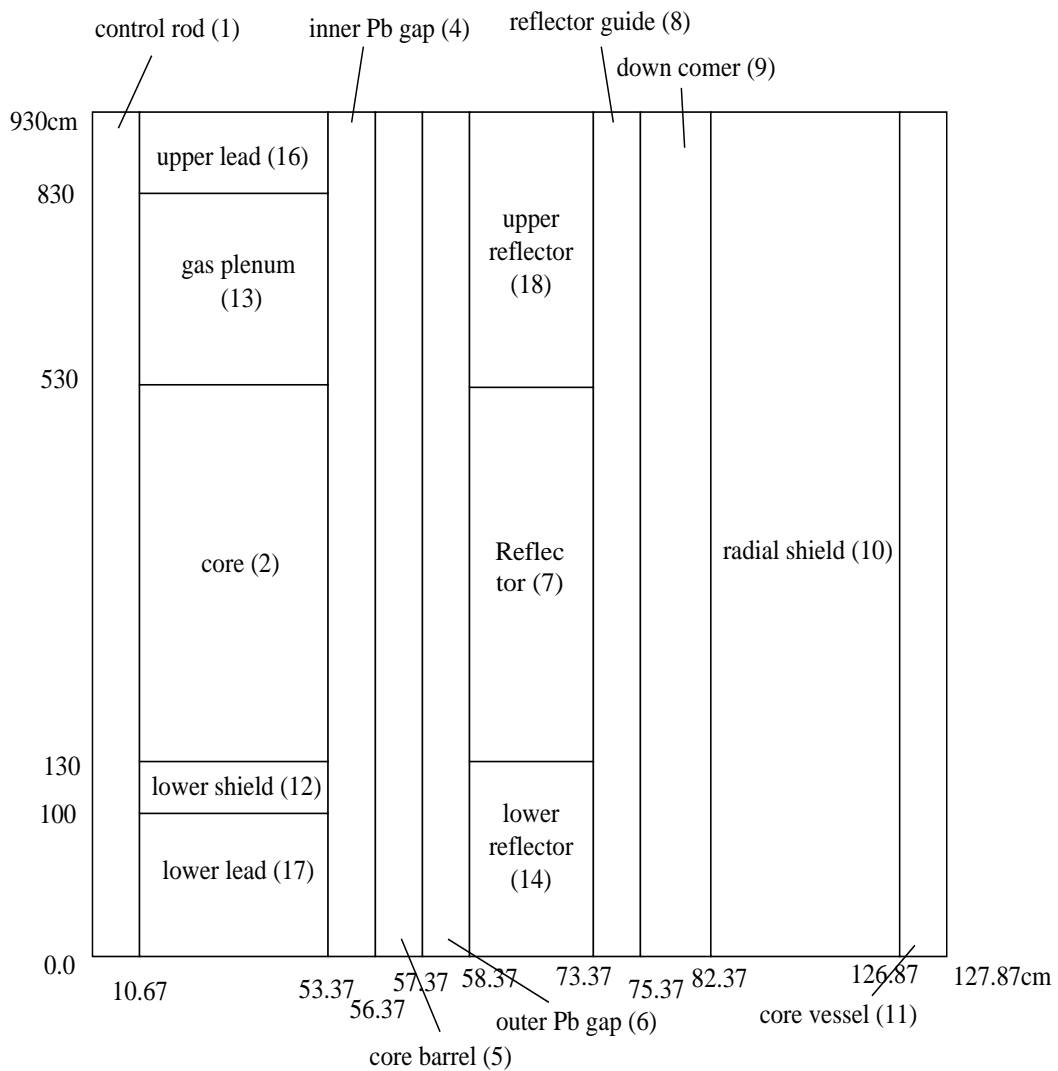


Figure1. ENHS benchmark problem geometry and dimensions

Table I. Material Composition, Volume Fraction and Temperature

Regions (region number)	Material; Volume fraction	Temperature (K)
Control rod region (1)	99%Pb + 1%SS	753
Core (2)	47.621%fuel+31.4253%Pb +20.953%SS	753
Inner Pb gap (4); Core barrel (5)	100%Pb	753
Outer Pb gap (6)	100%Pb	693
Radial reflector (7)	100%Pb	693
Reflector guide (8)	70%Pb+30%SS	693
Down comer (9); Radial shield (10)	100%Pb	693
Core vessel (11); Lower shield (12)	100%SS	693
Gas plenum (13)	31.4253%Pb+20.953%SS	813
Lower reflector (14)	100%Pb	693
Upper Pb (16)	100%Pb	813
Lower Pb (17)	100%Pb	693
Upper reflector (18)	90%Pb+10%SS	693

Table II. Atomic Number Densities (atoms/barn-cm) for Composing Materials

Regions (region number)	Atomic number density
Control rod region (1)	Pb : 3.02043E-2, Fe : 5.55118E-4, Ni : 1.14172E-4, Cr : 1.56540E-4, Mo : 1.37239E-5, Mn : 1.30727E-5
Core (2)	Pu-239 : 9.40189E-4, Pu-240 : 3.02336E-4 Pu-241 : 8.87696E-5, Pu-242 : 6.49405E-5 U-235 : 2.32633E-5, U-238 : 1.14617E-2 Zr : 3.73749E-3, Pb : 9.58770E-3, Fe : 1.16316E-2, Ni : 2.39230E-3, Cr : 3.28003E-3, Mo : 2.87562E-4 Mn : 2.73916E-4
Inner Pb gap (4)	Pb : 3.05094E-2
Core barrel (5)	Fe : 5.55118E-2, Ni : 1.14172E-2, Cr : 1.56540E-2, Mo : 1.37239E-3, Mn : 1.30727E-3
Outer Pb gap (6)	Pb : 3.07187E-2
Reflector (7)	Pb : 3.07187E-2
Reflector guide (8)	Pb : 2.15031E-2, Fe : 1.66535E-2, Ni : 3.42517E-3, Cr : 4.69619E-3, Mo : 4.11718E-4, Mn : 3.92180E-4
Down comer (9)	Pb : 3.07187E-2
Radial shield (10)	Pb : 3.07187E-2
Core vessel (11)	Fe : 5.55118E-2, Ni : 1.14172E-2, Cr : 1.56540E-2, Mo : 1.37239E-3, Mn : 1.30727E-3
Lower shield (12)	Pb : 3.07187E-2
Gas plenum (13)	Pb : 9.52193E-3, Fe : 1.16316E-2, Ni : 2.39230E-3, Cr : 3.28003E-3, Mo : 2.87562E-4, Mn : 2.73916E-4
Lower reflector (14)	Pb : 3.07187E-2
Upper Pb (16)	Pb : 3.03001E-2
Lower Pb (17)	Pb : 3.07187E-2
Upper reflector (18)	Pb : 2.76468E-2, Fe : 5.55118E-3, Ni : 1.14172E-3, Cr : 1.56540E-3, Mo : 1.37239E-4, Mn : 1.30727E-4

\* Fuel density : 15.85\*0.75g/cc, SS density : 7.95g/cc,

\*\* Pb density : 11.3g/cc(solid), (11072-1.2\*T)/1000 g/cc(liquid), where T is from 400 to 700C

### 3. COMPUTATIONAL METHODS

#### 3.1 UCB

The main computational tool employed at UC Berkeley consists of MCNP[3] and ORIGEN2[4] interfaced by the MOCUP[5] driver. In addition to calculating  $k_{\text{eff}}$ , flux and power distribution, MCNP calculates effective one-group cross-sections for the fuel constituents specified in its input. These cross sections are used by ORIGEN2 for burnup analysis. For isotopes not included in the MCNP analysis, ORIGEN2 uses cross sections from its pre-processed standard libraries. For the present study the ORIGEN2 standard libraries used are number 312 for actinides and number 313 for fission products, both generated for LMFBR applications. Due to limitations of the number of tallies that can be handled by MCNP, only 67 fission products in addition to 45 actinides could be included in the input to MCNP. The fission products selected for inclusion in the MCNP calculations were those with the highest fractional absorption as calculated by ORIGEN2.

A modified procedure of interfacing MCNP and ORIGEN2 was developed at UCB to bypass the limitation on the number of fission products that can be handled by MCNP. In addition to the 67 fission products mentioned above, all other fission products for which we had cross sections in the MCNP format were specified in the input to MCNP and taken into account for the calculation of  $k_{\text{eff}}$  etc. However, MCNP did not generate the effective one group cross sections for these extra fission products. An algorithm was written to transfer into the MCNP input the number density of these extra fission products in addition to the number densities MOCUP was set to transfer from ORIGEN2 to MCNP. Using this new procedure we were able to account for an additional 111 fission products in the MCNP calculations.

The cross-sections used for MCNP calculations are taken from primarily the Vinca library[6]; they are based on ENDF-B/VI; they are based primarily on ENDF-B/VI data but, when missing, on JENDL3.2 and BROND2 data. The MCNP results used for actinide concentration, reflector worth and space dependent burnup and fast neutron fluence were calculated using temperature dependent ENDF-B/VI based library generated at Texas A&M.

Another computational tool checked by UCB is a variant of MOCUP in which KENO V.a[7] is used instead of MCNP. The major advantage to using KENO is the decrease in computation time by about a factor of 20 over MCNP. It uses the ENDF/B-V based 238 group cross section library of the SCALE-4.4 code package[8]. This library has cross sections for 186 fission products. The original MOCUP coupling modules were used along with the scale module KMART and two additional modules written at UCB to make the coupling between KENO and ORIGEN2.

#### 3.2 ANL

The REBUS-3 code system[9] was used at ANL for the benchmark calculations. The DIF3D code[10] was used with 230-energy group structure for calculating the space and energy dependence of the neutron flux using a finite-difference RZ diffusion theory method. Burnup chains spanning the range from  $^{232}\text{U}$  to  $^{248}\text{Cm}$  were considered. The multi-group cross sections are based on ENDF/B-V.2 data and were generated using the MC<sup>2</sup>-2 code[11]. Towards the end of this study MC<sup>2</sup> processed cross section library derived from ENDF/B-VI became available and was used for recalculating the  $k_{\text{eff}}$  evolution with burnup.

A resonance “screening” procedure was utilized to pre-process broad resonances into the MC<sup>2</sup>-2

“smooth data” library at the 2082 group level. Self-shielding effects of the remaining resonances were explicitly evaluated in MC<sup>2</sup>-2 using the narrow resonance approximation, allowing for Doppler broadening, scattering interference, and overlap with neighboring resonances. For individual core-region materials of given nuclide density and temperature, homogeneous ultra-fine-group flux calculations were performed using MC<sup>2</sup>-2. The consistent P1 method was used with group-independent buckling search for the fundamental mode spectrum using 2082 groups.

From the homogeneous ultra-fine (2082 energy groups) MC<sup>2</sup>-2 calculations, 230-group cross sections were generated for individual materials of given nuclide density and temperature as specifically for the ENHS benchmark problem at beginning-of-life (BOL). The effect of fission products was accounted for using lumped fission product cross-sections for five different fissionable isotopes. The lumps were created from cross-sections for 180 individual isotopes using fission yields for <sup>235</sup>U, <sup>238</sup>U, <sup>239</sup>Pu, <sup>240</sup>Pu and <sup>241</sup>Pu. The 230 group cross sections, generated specifically for the core region, were also used in all non-core regions.

### 3.3 KAERI

KAERI also used the DIF3D/REBUS-3 code system of ANL but with different cross-section library. For all isotopes excluding fission products KAERI used the ENDF/B-VI based 150 group library KAFAX-E66[12] (MATXS format). This 150-group set is used for BOL calculations. For fission products the starting point is an ENDF/B-VI based 80 group cross section library (MATXS format). 17 lumped fission products and one dummy isotope are used to model the 172 fission products for the following fissionable isotopes: <sup>235</sup>U, <sup>236</sup>U, <sup>238</sup>U, <sup>237</sup>Np, <sup>238</sup>Pu, <sup>239</sup>Pu, <sup>240</sup>Pu, <sup>241</sup>Pu, <sup>242</sup>Pu, <sup>241</sup>Am, <sup>242m</sup>Am, <sup>243</sup>Am, <sup>242</sup>Cm, <sup>243</sup>Cm, <sup>244</sup>Cm, <sup>245</sup>Cm, <sup>246</sup>Cm and one dummy isotope. The end-of-life (EOL) calculations were performed using an 80 group cross section set. The 80 group cross sections for other than fission product isotopes was prepared from the above mentioned 150 group library using an approximate 150 group neutron spectrum. The MATXS format nuclear libraries were transformed with the TRANSX code[13] into the ISOTXS format that can be used in DIF3D and in TWODANT[14]. TRANSX performs self-shielding using the constant escape cross section option.

The DIF3D code is set to solve the neutron diffusion equation in R-Z geometry using the finite difference option setting zero incoming current boundary conditions at the outer surface of the reactor. In addition, the TWODANT S<sub>N</sub> transport code is used with a 25 group cross section library to estimate the initial k<sub>eff</sub> of the benchmark problem.

The depletion analysis was performed using a 9-group cross-section set obtained by flux-volume averaging of the 80-group cross-sections for each of the nine equal volume burnup zones the core is divided into; three radial zones and three axial zones. Some burnup calculations were done using either a single core zone or three radial zones of equal radial thickness. Test burnup calculations were also done using a 80 group cross section library. More details about the KAERI methodology as can be found in [15, 16].

## 4. RESULTS

### 4.1 EIGENVALUE

Figure 2 compares the k<sub>eff</sub> evolution calculated using ENDF-B/VI based cross sections and considering a single burnup zone. There is very good agreement between the UCB and KAERI results

although the MOCUP calculated  $k_{eff}$  does not decline with burnup as pronounced as does the KAERI and, especially, ANL results. The ANL results are consistently ~ 1% lower.

Figure 3 compares the  $k_{eff}$  values calculated by ANL using multi-group cross section libraries derived from ENDF/B-V versus ENDF/B-VI libraries. It is seen that the results using the ENDF-B/V derived library are consistently higher by ~0.5%. This same figure also shows that the KENO/ORIGEN calculated  $k_{eff}$  (UCB) using ENDF/B-V derived cross sections is ~0.5% higher than  $k_{eff}$  calculated by REBUS (ANL) using ENDF/B-V derived cross sections. A comparison between the ENDF/B-VI and JEF2.2 libraries is given in references [15] and [16].

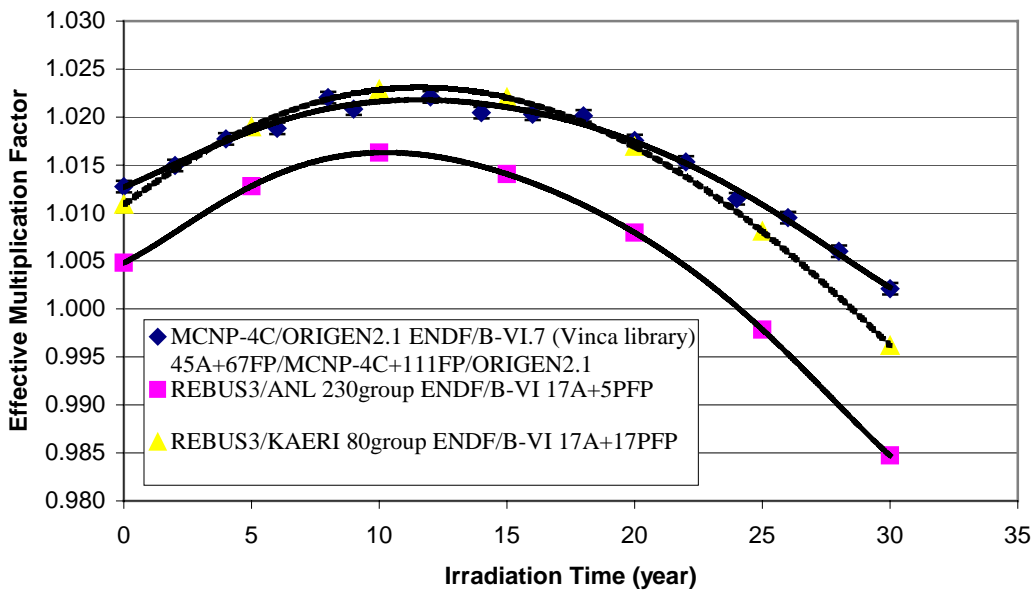


Figure 2.  $k_{eff}$  evolution in ENHS benchmark core obtained with different code systems using ENDF-B/VI based cross sections

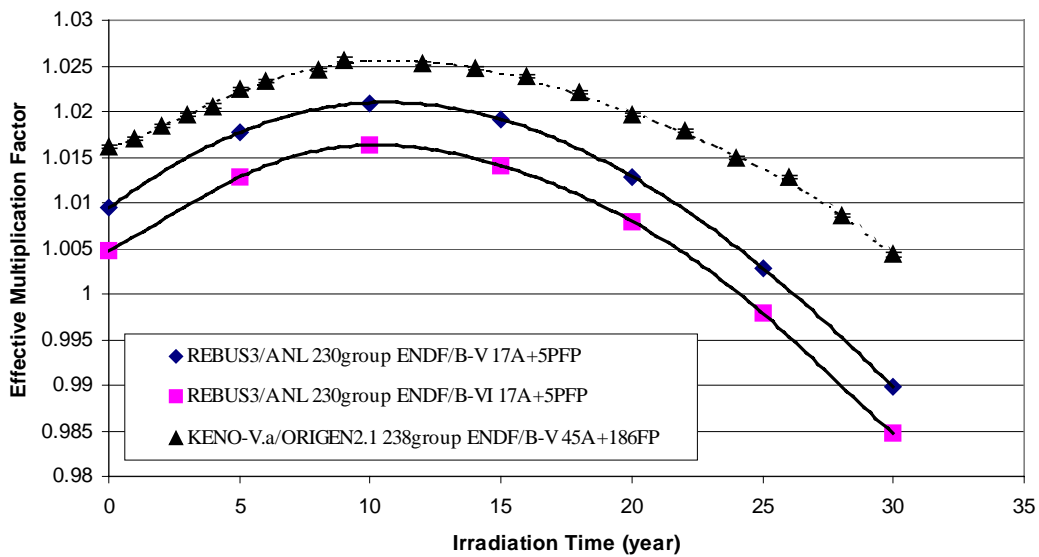


Figure 3. Effect of ENDF/B-V versus ENDF/B-VI on  $k_{eff}$  evolution in the ENHS benchmark

Figure 4 shows the effect on  $k_{eff}$  evolution of the handling of the fission products in the UCB MOCUP calculations. It is seen that accounting for the additional less-absorbing 111 fission products has a significant effect. The modified procedure for using MOCUP developed at UCB as a result of this benchmark study is valuable and will be used for future burnup analysis.

Figure 5 compares the effect on  $k_{eff}$  evolution with burnup of the number of burnup zones the core is divided into. It is found that for design work it is necessary to divide the core into several burnup zones; nine equal volume zones – 3 radial and 3 axial, were used in subsequent design studies.

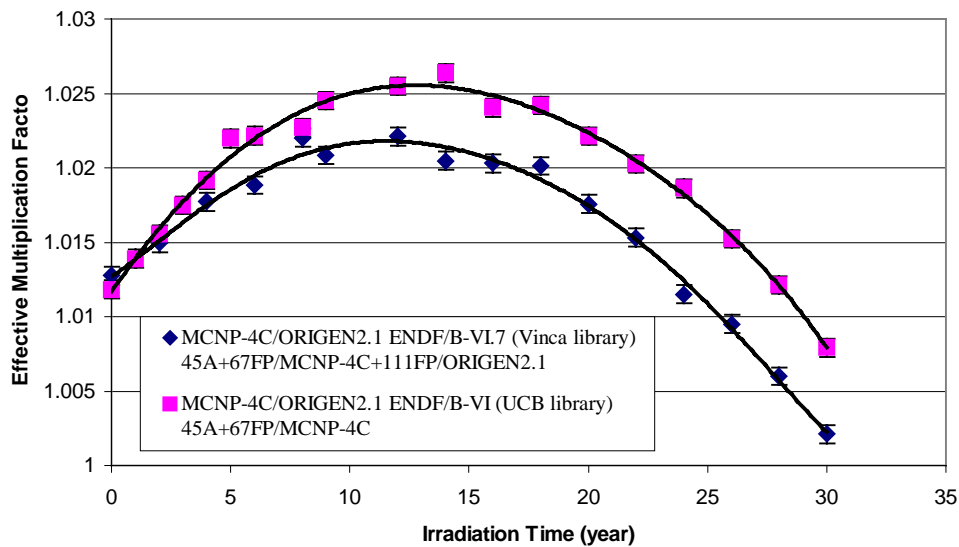


Figure 4. Effect of number of fission products on MOCUP calculated  $k_{eff}$  evolution in the ENHS benchmark

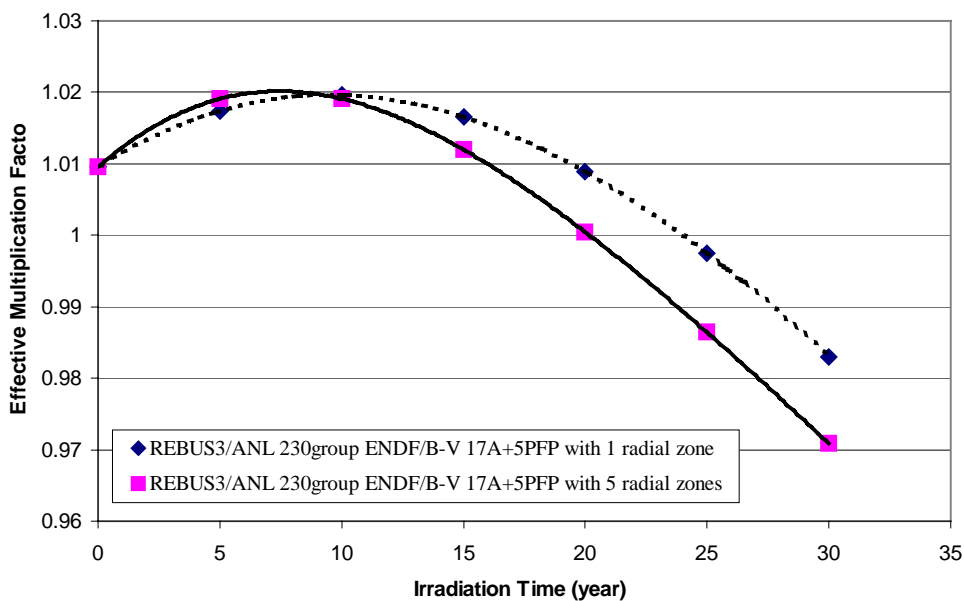


Figure 5. Effect of number of burnup zones on  $k_{eff}$  evolution in the ENHS benchmark

#### 4.2 EFFECTIVE ONE-GROUP CROSS-SECTION DATA

Figures 6 through 14 compare BOL effective one-group core-averaged cross-sections and  $\nu$  values. The ANL values in these charts come from ENDF/B-V while the UCB and KAERI values are based on ENDF/B-VI. Typical standard deviation of the MCNP generated values is ~0.2%. The results from KAERI for Neptunium and Curium isotopes are given after one year of burnup. It is expected that these values are very close to the corresponding BOL values, as the spectral shift in the ENHS during one year is expected to be negligible. The values for average number of neutrons released from fission show good agreement, less than ~0.1% difference, for the uranium and plutonium isotopes (Figures 6 and 7). There are larger discrepancies, up to ~7.0%, in the curium isotopes (Figure 8).

There is a very good agreement, to within ~2%, in the capture cross-section for the major uranium ( $^{235}\text{U}$  and  $^{238}\text{U}$ ) and Pu isotopes. There is not so good agreement for the curium isotopes; the worst agreement of >50% is for  $^{242}\text{Cm}$ . The fission cross-sections, Figures 12 to 14, show a similar trend.

#### 4.3 CORE COMPOSITION DATA

Table III shows the ratio of atomic number density calculated by ANL and UCB as a function of time. Whereas there is a very good agreement in the concentration of the primary uranium ( $^{238}\text{U}$  and  $^{235}\text{U}$ ) and plutonium ( $^{239}\text{Pu}$ ,  $^{240}\text{Pu}$ ,  $^{241}\text{Pu}$  and  $^{242}\text{Pu}$ ) isotopes, there is a significant discrepancy in the concentration of other fuel isotopes. Part of the discrepancy is probably due to the difference in the recoverable energy per fission discussed above. This discrepancy is expected to show up only for fuel isotopes the concentration of which vary with burnup significantly, such as for  $^{238}\text{Pu}$  and the minor actinides. The concentration of the major Pu isotopes and of  $^{238}\text{U}$  does not vary much.

#### 4.4 BURNUP AND FAST NEUTRON FLUENCE DISTRIBUTION

Tables IV and V compare, respectively, the burnup and the fast neutron fluence calculated as a function of time by the ANL, KAERI and UCB computational tools. For these calculations the core is divided into 3 radial zones. It is observed that, for the same operating time, MOCUP gives somewhat higher peak fast neutron fluence at the outer region and somewhat lower fluence at the inner region. This trend may be due to the difference in the method used for solving the transport equation: transport solution by MCNP (UCB) versus diffusion theory approximation by DIF3D (ANL & KAERI). Surprisingly, this trend is not observed in the space dependent burnup distribution. The burnup mismatch may be due in part to different value assumed for the average recoverable energy generated per average fission reaction; the UCB value is the smaller. The overall level of agreement seen between various tools on burnup and fast neutron fluence calculations is satisfactory for a feasibility study.

#### 4.5 REFLECTOR REACTIVITY WORTH

The reactivity worth at BOL of replacing the lead reflector, region 7 in Figure 1, by a "cavity reflector" is calculated to be -2.11% by MOCUP (UCB) versus -2.99% by REBUS3 (ANL). The "cavity reflector" is made of 10 volume % SS; the rest is void. The discrepancy between the ANL and UCB results is significant; it is much larger than the statistical uncertainty in MOCUP (< 1%). This discrepancy is due, in part to the inadequacy of the diffusion approximation (DIF3D) to account for neutron transport in void.



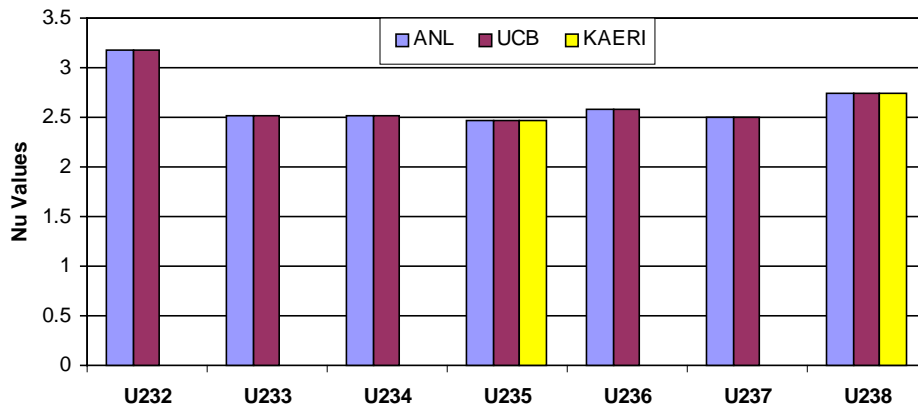


Figure 6.  $\nu$  value comparison for uranium isotopes

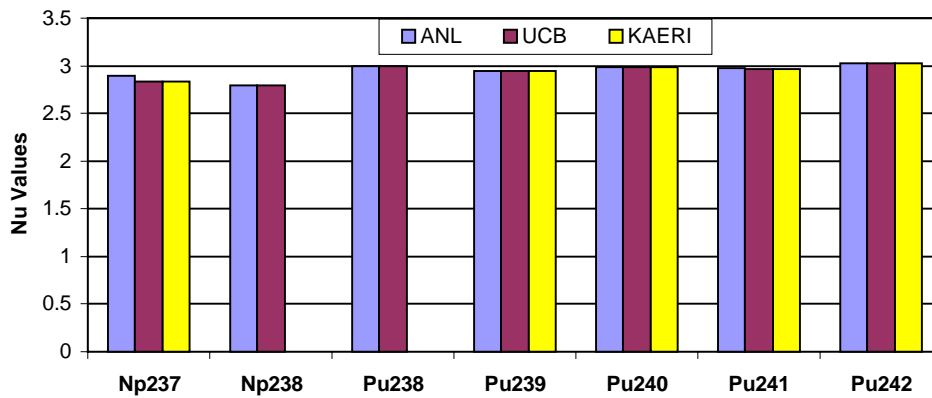


Figure 7.  $\nu$  value comparison for plutonium and neptunium isotopes

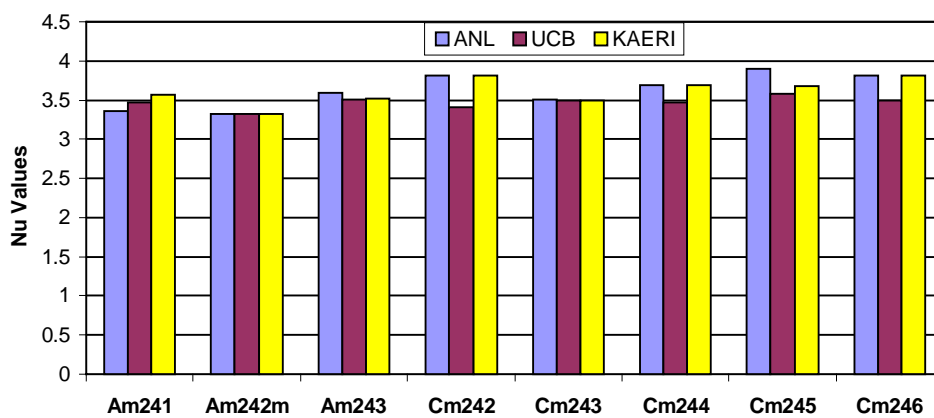


Figure 8.  $\nu$  value comparison for americium and curium isotopes

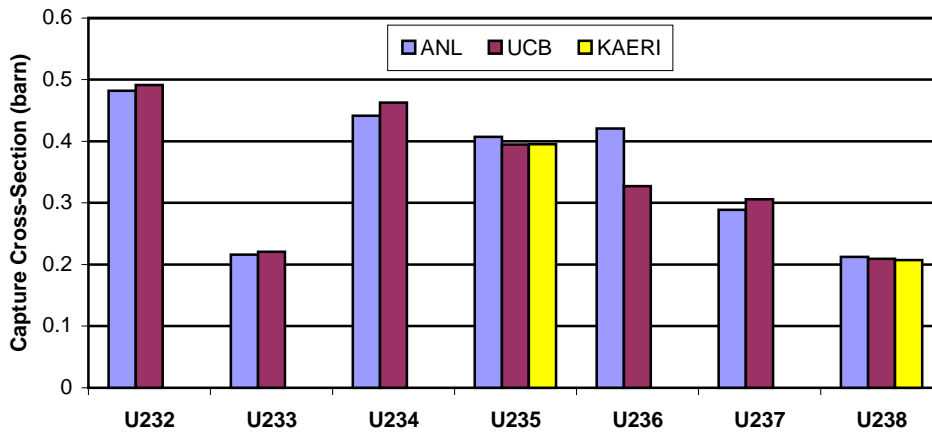


Figure 9. Capture cross-section comparison for uranium isotopes

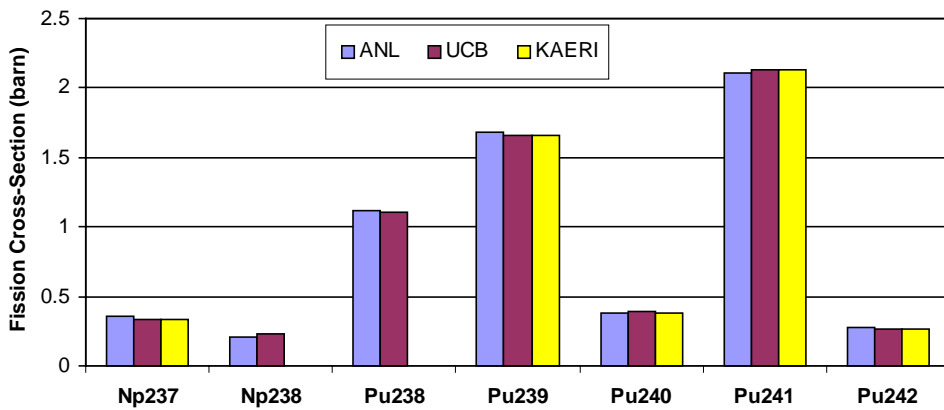


Figure 10. Capture cross-section comparison for plutonium and neptunium isotopes

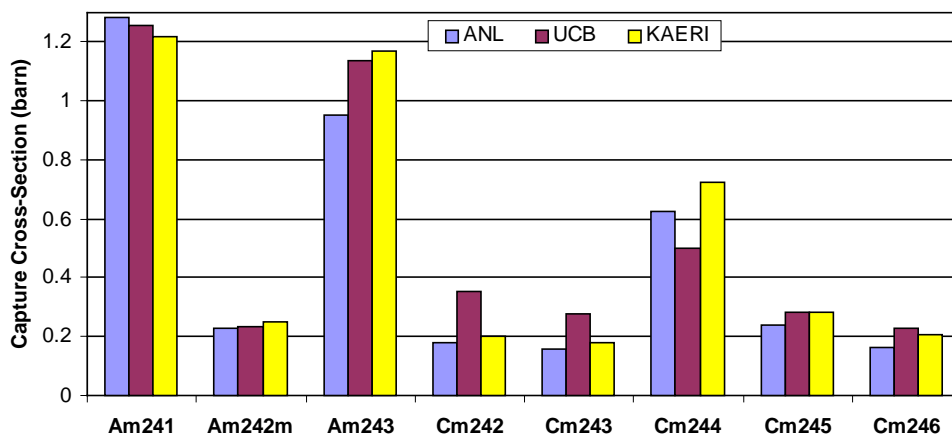


Figure 11. Capture cross-section comparison for americium and curium isotopes

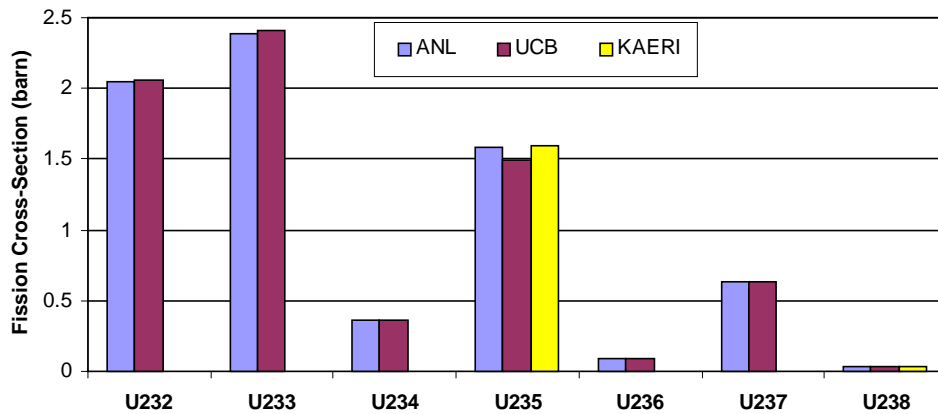


Figure 12. Fission cross-section comparison for uranium isotopes

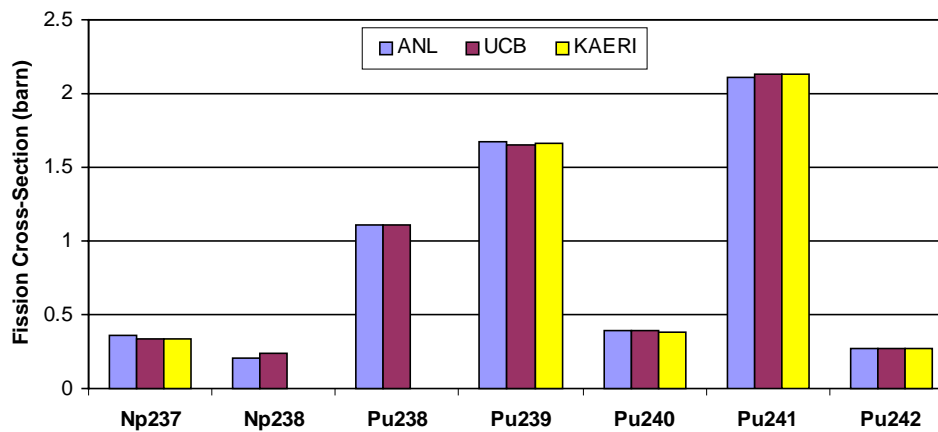


Figure 13. Fission cross-section comparison for plutonium and neptunium isotopes

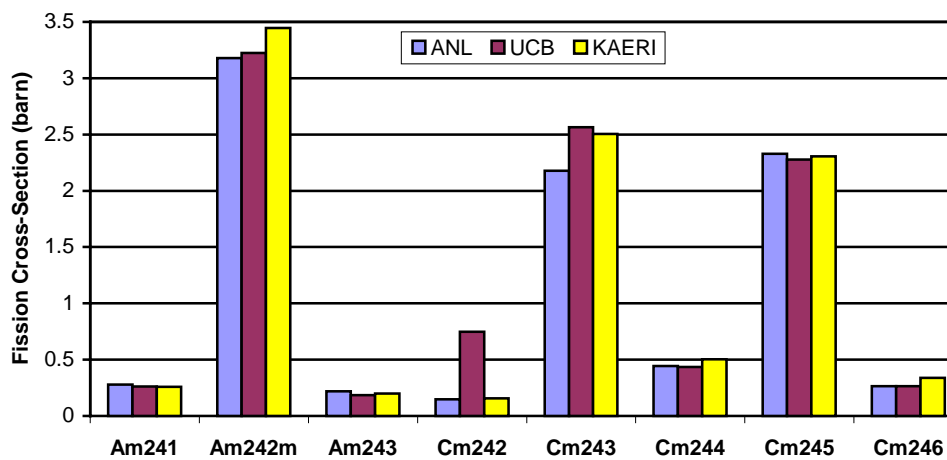


Figure 14. Fission cross-section comparison for americium and curium isotopes

Table III. Ratio of Atomic Number Density: ANL/UCB

Isotope	0 years	5 years	10 years	15 years	20 years	25 years	30 years
U232	1.00	0.96	0.74	0.44	0.24	0.13	.072
U233	1.00	0.98	0.90	0.79	0.66	0.57	0.52
U234	1.00	0.80	0.84	0.86	0.87	0.88	0.90
U235	1.00	1.00	1.00	1.01	1.01	1.01	1.01
U236	1.00	1.01	1.00	0.99	0.99	0.98	0.97
U237	1.00	1.08	1.06	1.07	1.04	1.05	1.07
U238	1.00	0.99	1.00	1.00	1.00	1.00	1.00
Np237	1.00	1.06	1.06	1.06	1.05	1.05	1.06
Np238	1.00	1.06	1.06	1.05	1.04	1.04	1.04
Pu238	1.00	0.83	0.86	0.87	0.89	0.90	0.92
Pu239	1.00	1.00	1.00	1.00	1.00	1.00	1.00
Pu240	1.00	1.00	1.00	1.00	1.00	1.01	1.01
Pu241	1.00	1.01	1.02	1.03	1.04	1.04	1.04
Pu242	1.00	1.00	1.00	1.00	1.00	1.00	1.01
Am241	1.00	1.00	1.03	1.05	1.06	1.08	1.10
Am242m	1.00	0.89	0.90	0.92	0.93	0.94	0.96
Am243	1.00	1.05	1.11	1.18	1.24	1.30	1.36
Cm242	1.00	0.83	0.85	0.87	0.88	0.90	0.91
Cm243	1.00	0.78	0.79	0.81	0.82	0.84	0.85
Cm244	1.00	0.52	0.54	0.57	0.59	0.61	0.63
Cm245	1.00	0.49	0.50	0.51	0.52	0.53	0.54
Cm246	1.00	0.75	0.53	0.51	0.52	0.52	0.53
Cm247	1.00	1.00	0.92	0.70	0.57	0.53	0.52
Cm248	1.00	1.00	1.00	0.99	0.97	0.92	0.83

Table IV. Time-Dependent Integrated Average Burnup [atomic percent]

Time (year)	Inner Region			Middle Region			Outer Region			Core Average		
	ANL	KAERI	UCB	ANL	KAERI	UCB	ANL	KAERI	UCB	ANL	KAERI	UCB
5	3.17	3.35	3.5	2.63	2.94	2.96	2.2	2.31	2.52	2.66	2.71	2.99
10	6.33	6.71	6.65	5.25	5.87	5.57	4.4	4.63	4.71	5.33	5.43	5.64
15	9.47	10.05	9.79	7.87	8.79	8.17	6.62	6.97	6.9	7.99	8.15	8.29
20	12.59	13.36	12.92	10.48	11.71	10.77	8.86	9.32	9.12	10.64	10.87	10.94
25	15.68	16.65	16.01	13.1	14.62	13.38	11.11	11.69	11.36	13.3	13.59	13.58
30	18.74	19.92	19.07	15.72	17.53	15.99	15.95	14.08	13.62	15.95	16.31	16.23

Table V Core Region Peak Fast Neutron Fluence(<0.1MeV),  $10^{23}$  [n/cm<sup>2</sup>]

Time (year)	Inner Region			Middle Region			Outer Region			Core Average		
	ANL	KAERI	UCB	ANL	KAERI	UCB	ANL	KAERI	UCB	ANL	KAERI	UCB
5	1.9	1.83	1.61	1.59	1.7	1.33	1.2	1.3	1.34	1.56	1.53	1.43
10	3.79	3.67	3.31	3.16	3.4	2.71	2.39	2.6	2.74	3.11	3.06	2.92
15	5.67	5.46	5.01	4.73	5.07	4.11	3.57	3.88	4.15	4.66	4.57	4.42
20	7.55	7.2	6.62	6.3	6.69	5.45	4.77	5.12	5.49	6.21	6.03	5.85
25	9.43	8.9	8.22	7.89	8.27	6.78	5.98	6.34	6.83	7.77	7.46	7.28
30	11.3	10.58	9.86	9.5	9.85	8.12	7.2	7.56	8.19	9.35	8.89	8.72

## 5. CONCLUSIONS

The overall agreement between the computational tools used at UCB, ANL and KAERI for the ENHS benchmark is satisfactory. In particular, the disagreements found would not affect the conclusions concerning the feasibility of designing the ENHS core to have a nearly constant  $k_{\text{eff}}$  for 20 effective full power years. The neutronic characteristics of the ENHS reactor can be predicted with accuracy that is sufficient for assessing the feasibility of this reactor concept. Nevertheless, it is desirable to resolve the discrepancy in prediction of  $k_{\text{eff}}$  between the ANL and between KAERI and UCB. It is also desirable to resolve the discrepancy in the value of capture and fission cross sections for some of the minor actinides, primarily higher Cm isotopes. The apparent inconsistency between the space dependent burnup and fast neutron fluence distributions need be understood as well. For accurate calculations it is necessary to account for more than 67 fission products (preferably ~ 180) and to divide the core into at least 9 regions for performing the burnup analysis.

## REFERENCES

1. E. Greenspan, N. W. Brown, M. D. Carelli, L. Conway, M. Dzodzo, Q. Hossain, D. Saphier, J. J. Sienicki, D. C. Wade, "The Encapsulated Nuclear Heat Source Reactor – A Generation IV Reactor," *Proc. of GLOBAL-2001*, Paris, France, September 2001.
2. E. Greenspan, N. W. Brown, M. D. Carelli, L. Conway, M. Dzodzo, Q. Hossain, D. Saphier, J. J. Sienicki, D. C. Wade, "The Encapsulated Nuclear Heat Source Reactor for Proliferation-Resistant Nuclear Energy," *Proc. of GLOBAL-2001*, Paris, France, September 2001.
3. J. F. Briesmeister, Ed., "MCNP – A General Monte Carlo N-Particle Transport Code", *Los-Alamos National Laboratory Report LA-12625-M, Version 4B* (1997).
4. A. G. Croff, "ORIGEN2 - A Revised and Updated Version of the Oak Ridge Code," *Oak Ridge National Laboratory Report ORNL/TM-7175* (1980).
5. R. L. Moore et al., "MOCUP:MCNP-ORIGEN2 Coupled Utility Program," *Idaho National Engineering Laboratory Report INEL-95/0523*, 1995.
6. M. J. Milosevic, "The VMCCS Data Library for MCNP," *Vinca Institute of Nuclear Science Bulletin*, **3**, No. 1-4, pp. 11-14, 1998.
7. D. F. Hollenbach, L. M. Petrie and N. F. Landers, "KENO-VI: A General Quadratic Version of the KENO Program," *NUREG/CR-0200, Revision 5, Volume 2, Section F17*,

- ORNL/NUREG/CSD-2/V2/R5, (September 1995).
8. "SCALE-4.4a: A Modular Code System for Performing Standardized Computer Analyses for Licensing Evaluation," *NUREG-CR-0200, Rev.5, Oak Ridge National Laboratory*, September 1998.
  9. B. J. Toppel, "A User's Guide for the REBUS-3 Fuel Cycle Analysis Capability," *Argonne National Laboratory Report ANL-83-2*, (Mar. 1983).
  10. K. L. Derstine, "DIF3D: A Code to Solve One-, Two-, and Three-Dimensional Finite Difference Diffusion Theory Problems," *Argonne National Laboratory Report ANL-82-64*, (1982).
  11. H. Henryson, II, B. J. Toppel, and C. G. Stenberg, "MC2-2: A Code to Calculate Fast Neutron Spectra and Multigroup Cross Sections," *Argonne National Laboratory Report NL-8144* (June 1976).
  12. J. D. Kim, "KAFAX-E66", *Calculation Note No. NDL-23/01, KAERI Nuclear Data Evaluation Lab. Internal Report* (2001).
  13. R. E. MacFarlane, "TRANSX 2 : A Code for Interfacing MATXS Cross-Section Libraries to Nuclear Transport Codes," *LANL Report, LA-12312-MS* (December 1993).
  14. R. E. Alcouffe, *et al.*, "User's Guide for TWODANT: A Code Package for Two-Dimensional Diffusion-Accelerated, Neutral-Particle Transport," *LANL report, LA-10049-M* (1984).
  15. S. G. Hong and Y. I. Kim, "Comparison of the ENDF/B-VI and JEF2.2 Nuclear Data for the ENHS Benchmark Problem," *Trans. Amer. Nucl. Soc. Mtg*, **85**, 111, Reno, NV, Nov. 11-15, 2001.
  16. S. G. Hong and Y. I. Kim, "A Comparative Neutronics Analysis by Using Two Different Nuclear Libraries for the ENHS Core Benchmark Problem," *Proc. of Int. Conf. On New Frontiers of Nuclear Technology: Reactor Physics, Safety and High Performance Computing, PHYSOR-2002*, Seoul, Korea, Oct. 7-10, 2002.